Escola de Camins
Escola Tècnica Superior d'Enginyeria de Camins, Canals i Ports
UPC BARCELONATECH

TREBALL FINAL DE GRAU

# Simulation of Mass-less Oscillations in Biological Tissues with Delay Differential Equations


Treball realitzat per:
**Mònica Dingle Palmer**

Dirigit per:
**José J. Muñoz**

Grau en:
**Enginyeria Civil**


Barcelona, 15 de juny del 2018


MAT – Departament de Matemàtiques

# Contents

# List of Figures

# Abstract

It has been observed that during early stages of embrionic developement, tissues oscillate in a fluid-like manner. This behaviour is surprising because PDEs that simulate the latter do not present an apparent oscillatory solution, fact that might imply that oscillations' sources could be given by the coupling between mechanical equilibrium and the biological/chemical response of the cells. In this work, the main objective is to prove that these oscillations can indeed emerge if a delay which represents the time that the system needs to respond to mechanical events due to chemical signalling is implemented in the model. In addition, stability of such oscillations is studied, because resonance effects appear even though no external forces are applied on the system, pointing that the delay might be responsible for that too. The main aim of this stability analysis is to be able to obtain the stability diagram of one element and two element systems and therefore to characterize its behaviour as a function of its parameters.

**Keywords**: *oscillations, stability, time delay, delay differential equations, active lengthening model, method of characteristics*

# Chapter 1

# Introduction

## 1.1 General background

### 1.1.1 Cytoskeleton

Being cell movements, deformations and displacements the main scope of this work, it is important to start the contextualization by providing some information about the agents involved in this processes. In this case, the ultimate responsible for a cell movement is its cytoskeleton.

The cytoskeleton is a structure that helps cells maintain their shape and internal organization, providing mechanical support that enables them to carry out their essential functions such as division or movement. Several components structure it in the case of eukaryotic cells, but filamentous proteins are the ones that assume the role as supporters of the cell and its cytoplasmic constituents. Depending on the size and protein composition, three main types are to be found;

- Microtubules: they are the largest type, composed by a protein called tubulin.
- Intermediate filaments: as their name suggests, they are intermediate sized, and composed by many different proteins.
- Actin filaments: they are the smallest type, constructed by a protein called actin.

In the next figure cytoskeletal filaments that provide the basis for cell movement are shown.

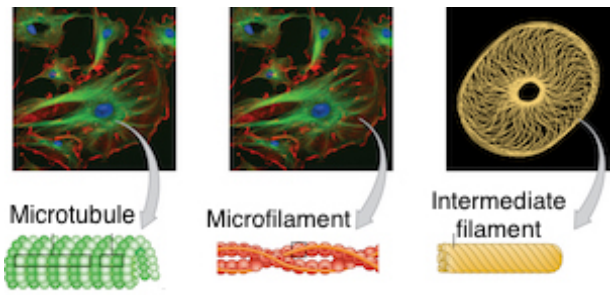


Figure 1.1: Detail of the cytoskeletal filaments. (https://study.com/academy/lesson/cytoskeletal-proteins-types-function.html)

### 1.1.2 Morphogenetic events in embryonic development

Morphogenesis is a biological process that causes the organism to develop its shape. These type of events might be triggered by hormones, different types of chemicals to which the developing organisms might be exposed to, or mechanical stresses induced by the spatial patterns that cells follow. This work focuses on the latter, and tries to comprehend the behaviour of the displacements that are produced by such forces and whom drive morphogenetic events.

Among all possible morphogenetic events, our scope will be embryonic development. The reason why it has become an interesting field of study is because before the drastic tissue rearrangements occur and the organism and its organs are shaped, tissues' deformations oscillate in a fluid-like manner, a type of behaviour that is surprising because equations that model such demeanour do not take into account inertial terms, resulting in an elliptical or parabolic PDE with no apparent oscillatory solution. Therefore, one of the main purposes of this work is to study the coupling between mechanical equilibrium and biochemical coupling as a possible source of oscillations.

As it has been stated in the previous paragraphs, dramatic tissue rearrangements that lead to the posterior shaping of the organism happen during the early stages of embryonic development. The complex signalling networks that are sequentially activated to coordinate such movements have been uncovered by genetic studies, but the origin and nature of the forces that drive these changes in space and time has not been entirely clarified yet, mainly due to the difficulty of directly measuring these type of magnitudes in living organisms. To add even more complication to the issue that is being addressed, it should be taken into account that finding underlying force in a moving system can also be challenging, because neighbouring systems could also be affected by it. Regardless of such difficulties, some experiments have addressed the issue by using real time fluorescence imaging and laser incisions to release tension [1], enabling the description of these forces.

### 1.1.3 Dorsal closure

Amid the possible processes to be studied, dorsal closure in the early stages of the *Drosophila melanogaster* embryo is the one that this work focuses on. It consists of the closure of an opening in the embryo's dorsal epidermis, a type of rearrangement of tissues that is interesting due to its resemblance to wound healing processes [2].

These two processes, which at first glance do not resemble that much, have many things in common. They both start with the activation of the Jun N-Terminal kinase (mitogen activated protein kinases) signalling pathway, which prompts the formation of the suppracellular actin cable in the row of epidermis cells at the leading edge of the opening, which is constricted by the fore-mentioned cable. While the dorsal closure takes place, the cells of the amnioserosa tissue that fill the opening cooperate with the actin cable by providing additional contractile forces that appear due to the decrease of the apical surface of the amnioserosa cells, pulling the leading edges towards the dorsal midline [3].

Once the leading edges are close enough, and the amnioserosa cells have reached their maximal contraction potential [4], protrusions will start to grow on the edges, and by find-

ing an impaired protrusion on the opposite edge, a zippering-like mechanism will start to close the gap and push the amnioserosa cells down.

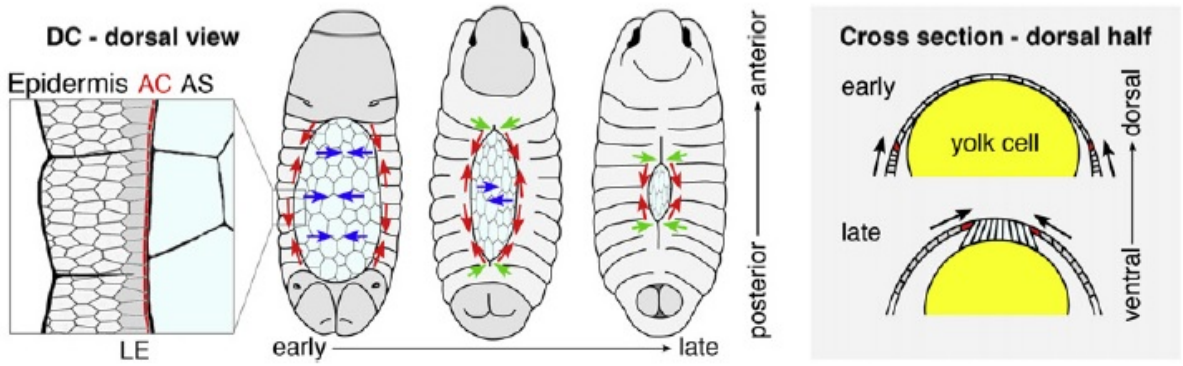


Figure 1.2: Cartoon of DC embryos. Colored arrows depict forces produced by AS cells (blue), AC (red), and zippering (green). Black arrows show the direction of LE movement. [5]

### 1.1.4 Pulsing as an intrinsic property of amnioserosa cells

Recent investigations have demonstrated that the forces exerted by the amnioserosa cells are not gradual, but pulsed. In addition, it has also been proved that this pulsing behaviour starts long before dorsal closure does, proving that it is an intrinsic property of such cells and is coordinated within the tissue by a tension based mechanism.

Individual cell geometries were studied using automated image segmentation technology, and the conclusion was that they contracted their apical surfaces with a given periodicity, raising the question of how this contractions are correlated with the overall contraction of the cell surface while dorsal closure takes place. Further investigations have shown that amnioserosa cells reach their minimal apical surface when fully contracted, but their maximal extension remains constant until the beginning of the closure and from that point, they decrease. This decrease in the apical surface is the result of the reduction in pulsing amplitude, which continues until there is a complete arrest of such pulsations. Therefore, final results of the investigation show that during dorsal closure, apical surface constriction of the amnioserosa cells is a consequence of the damping of the pulsations, which is coordinated in space and time with the pulsation arrest [5].

Finally, studies that correlate such pulsations with neighbouring elements (leading edge and actin cable) conclude that these oscillations require from tissue tension as well as from biological coupling, which directly points at the presence of a mechanical control that couples their behaviour. Still, the exact biophysical process is yet unknown.

## 1.2 Modelling of the tissue

In order to simulate the tissues and study their behaviour thoroughly, a model is needed. There are two main types of them, the Continuum ones and the vertex or cell-centered

ones. In the first ones, constitutive behaviour of the system is described [6] and discretized using techniques such as finite elements [7] [8]. Vertex and cell-based models instead can represent junctional mechanics and it is capturing the discrete and cellular characteristics of tissues [9] [10] [11]. This is the model that is used in this approach.

The proposed one is a network of visco-elastic polygons with shared edges and where vertexes are connected to the cell's center of mass, an idealization that has been used in previous studies [12].

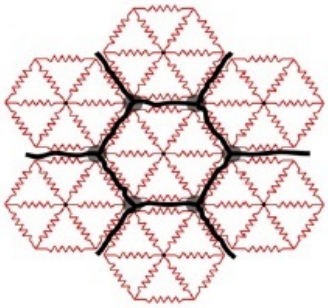

Figure 1.3: The geometry and spring distribution of AS cells is shown. In every cell, elastic springs (red) connect all neighboring vertices (gray dots) and each vertex with the center of mass. Black lines depict cell boundaries. [5]

In chapter 4, a hybrid model developed by Muñoz, J., Rodríguez-Ferran, A. and Albo, S. [17] is shown.

## 1.3 Motivation and objectives

After many years in an engineering school, it is a personal challenge to use my acquired skills in a field which is completely new to me. To be able to participate in a project that blends biology, physics and numerical modelling has been a mind opening opportunity, giving me the chance to discover new fields where the concepts that were taught to me during my degree could be of some use, and of course, to learn new ones in this field called biomechanics.

The objective of this project is to study the behaviour of the oscillations that take place during embryonic development by using a model called Active Lengthening Model, proposed by Muñoz, J. and Albo, S. [13]. General objectives are:

- Solve the equations that compose the model.
- Study the solutions of the equation as a function of its parameters.
- Find critical values of the parameters where oscillations appear.
- Define stability limits as a function of those parameters.

This analysis will be carried on 1-element (1-E) and 2-element (2-E) models. Special attention will be paid to the 1-E model, because its behaviour could determine the 2-E model responses too. To reach the goals that have been stated, a variety of analytical

tools and methods will be used in order to obtain analytical solutions and values, but numerical methods will also be needed and will play a major role in this project.

## 1.4 Active lengthening model

### 1.4.1 Strain based model

The strain based model that describes the behaviour of the tissue was introduced by Muñoz, J. and Albo, S., as stated before. An evolution law of the remodelling process in the cytoskeleton models the viscous properties of biological cellular tissues, based on the dynamical changes of the resting length of each element, which is idealized as a spring.

The equation that was initially proposed is the following one:

$$\frac{\dot{L}(t)}{L(t)} = \gamma\varepsilon(t) \tag{1.1}$$

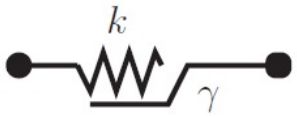


Figure 1.4: Representation of the proposed elastic element with changing resting length [13]

where $\varepsilon = \dfrac{(l(t) - L(t))}{L(t)}$, being $L(t)$ the current resting length of the combined filaments (length when no loads are applied on the ends), $l(t)$ the total length of them, and $\gamma$ a parameter called *remodelling rate* which represents the resistance of the network to adapt its configuration to the new imposed deformation.

Physical interpretation of this model is the following. A set of cross-linked actin filaments, under macroscopic strains, stretch as a result of a reversible (elastic) deformation and a non-reversible remodelling and lengthening, which could be explained as a the remodelling of the cross-links and the (de)polymerization process of the filaments in the cytoskeleton [13].

But the evolution law that was initially proposed was modified by the same authors to better describe the behaviour of such systems. A contractility parameter $\varepsilon_c$ (elastic strain at which no changes occur) was added due to the fact that cells are permanently under contractions generated from myosin [14], and a delay parameter $\tau$ was also added because oscillations could be the result of the time delayed response of mechanical events on chemical signalling. Therefore, the new evolution law reads:

$$\frac{\dot{L}(t)}{L(t)} = \gamma(\varepsilon(t - \tau) - \varepsilon_c) \tag{1.2}$$

It has been shown that combining changing resting length with an elastic law, the resulting model is equivalent to a Maxwell model.

### 1.4.2 Displacement based model

In this project, the model that will be used is not strain based, but displacement based. It is a rheological model which is slightly simplified, with no contractility parameter. The evolution law, in this case, reads;

$$\dot{L} = \gamma(l(t-\tau) - L(t-\tau)) \tag{1.3}$$

where $l(t)$, $L(t)$, $\tau$ and $\gamma$ are the same exact parameters as in equation (1.2).

As it can be seen, the resting length does not depend on $t$, but on $(t-\tau)$. This type of equations, where the function does not depend on the present instant of time but on a past instant, are known as *Delay Differential Equations*.

### 1.4.3 Delay Differential Equations

Some physical phenomenons take little time to process in comparison to the data-collection times, such as acceleration or deceleration, where we could say that response is almost instant. But in some other cases, such as biological systems, their response time is not so small in comparison to the data collection time. Therefore, this delay needs to be implemented into the mathematical model, just like the system this project is about.

Models that incorporate this delay time are called *Delay Differential Equations* (DDE's), differential equations in which the derivative of the unknown functions at present time depend on the values of the function at previous times. The general DDE equation takes the form;

$$\frac{dx(t)}{dt} = f(t, x(t), x(t-\tau_1), x(t-\tau_2), ..., x(t-\tau_n) \quad t \geq t_0 \tag{1.4}$$

$$x(t) = \phi_(t) \quad t \leq t_0 \tag{1.5}$$

where $\tau_i \geq 0,\ i = 1, ..., n$ are the time delays and $\phi(t)$ is the initial history function.

Applications of this models can be found in fields such as population dynamics, epidemiology, immunology, physiology, and neural networks among others.

# Chapter 2

# 1-element model

In this chapter, the 1-element model will be studied. Solutions to the problem will be found, and then, a stability analysis will be performed in order to find critical values of *gamma* and $\tau$ for which oscillations appear.

To perform such analysis, analytical and numerical methods will be used. The two main analytical ones are;

1. Step method: this method will be used to find an analytical solution to compare numerical results and check accuracy.
2. Characteristics method: this method is mainly used to find critical values for $\gamma$ and $\tau$.

Numerical methods (Forward Euler Method, Backward Euler Method) will be used to perform tests and check the behaviour of the oscillations once analytical values for critical $\gamma$ and $\tau$ are found.

## 2.1 1-element problem statement

As it has previously been stated, we will use the simplified Active Lengthening Model [13]. We will study its behaviour when a constant displacement $u$ is applied (figure 2.1):

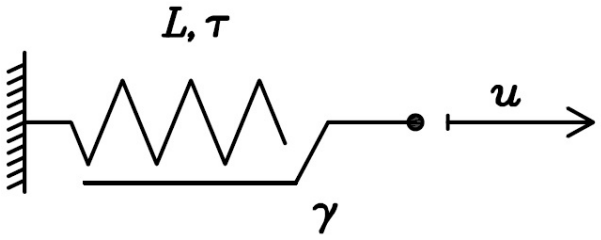


Figure 2.1: 1-element model.

Therefore, the DDE problem we have:

$$\begin{cases} \dot{L} = \gamma(l - L(t-\tau)), & t \geq 0 \\ L(t) = L_0, & t \in [-\tau, 0] \end{cases} \tag{2.1}$$

where $l = L_0 + u = ct,\ \gamma, \tau > 0$ are characteristic parameters of the system and therefore are given. Solutions of the problem (resting length $L(t)$) will be studied as a function of both of them.

## 2.2 Solutions to the 1-E problem

In this section, analytical and numerical solutions to the 1-E problem will be presented as a function of $\tau$ and $\gamma$, using two different methods: the Step Method (analytical) and numerical methods (Forward and Backward Euler).

*Note: to perform numerical tests, values for the different initial conditions will be $L_0 = 1$ and $l = 2$.*

### 2.2.1 Step Method

This method converts the DDE on a given interval to an ODE over that interval by using the known history function on that interval. The resulting equation is solved and the process is repeated on the next interval with the solution that has just been found being used as the history function over that interval [15]. As an example, let us consider the linear DDE with constant coefficients $a_1,\ a_2$ and constant delay $\delta$ along with the history function $\phi(t)$:

$$\begin{cases} \dfrac{dy(t)}{dt} = a_1 y(t) + a_2 y(t-\delta) & t \geq 0 \\ \phi(t) = p(t) & t \in [-\delta, 0] \end{cases} \tag{2.2}$$

**Step 1**. On the first interval, $y(t) = \phi(t),\ \forall t \in [-\delta, 0]$ so on this interval, $y(t)$ is already solved, and we'll denote it by $y_0(t)$

**Step 2**. On the next interval, $y(t-\delta) = y_0(t-\delta),\ \forall t \in [\delta, 0]$, therefore, the resulting ODE plus its boundary condition reads:

$$\begin{cases} \dfrac{dy(t)}{dt} = a_1 y(t) + a_2 y(t-\delta) = a_1 y(t) + a_2 y_0(t-\delta), & t \in [\delta, 0] \\ y(0) = \phi(0) \end{cases} \tag{2.3}$$

which can easily be solved. Let's call $y_1(t)$ the solution for this time step.

**Step 3.** On the next interval, $y(t-\delta) = y_1(t-\delta)$, $\forall t \in [\delta, 2\delta]$, therefore, the next problem reads:

$$\begin{cases} \dfrac{dy(t)}{dt} = a_1 y(t) + a_2 y(t-\delta) = a_1 y(t) + a_2 y_1(t-\delta), \quad t \in [\delta, 2\delta] \\ y(\delta) = y_1(\delta) \end{cases} \tag{2.4}$$

which can be solved, denoting the solution as $y_2(t)$.

Repeating this process for $n$ necessary time steps, the solution for the DDE is a stepwise function defined by the solutions $y_n(t)$ calculated at each time step. By proceeding this way, we obtain an analytical solution for our DDE, which can be used to check our numerical results and to check the behaviour of the equation for some given parameters.

Applying this procedure to problem (2.1):

**History function.** According to (2.1), the problem is solved in $t \in [-\tau, 0]$:

$$L_0(t) = L_0, \quad t \in [-\tau, 0] \tag{2.5}$$

**Step 1.** On the next time interval $[0, \tau]$, we have that $L(t-\tau) = L_0(t-\tau)$, therefore, we can write;

$$\begin{cases} \dot{L_1}(t) = \gamma(l - L(t-\tau)) = \gamma(l - L_0(t-\tau)) = \gamma(l - L_0), \quad t \in [0, \tau] \\ L_1(0) = L_0(0) \end{cases} \tag{2.6}$$

Solving this ODE, we obtain:

$$L_1(t) = \gamma(l - L_0)t + c_1$$

and applying boundary conditions $L_2(0) = L_1(0)$, we obtain:

$$\boxed{L_1(t) = \gamma(l - L_0)t + L_0} \tag{2.7}$$

**Step 2.** On the next time interval $[\tau, 2\tau]$, $L(t-\tau) = L_1(t-\tau)$, thus, we have the following problem:

$$\begin{cases} \dot{L_2}(t) = \gamma(l - L(t-\tau)) = \gamma(l - L_1(t-\tau)) = \gamma(l - (\gamma(l - L_0)t + L_0)), \quad t \in [\tau.2\tau] \\ L_2(\tau) = L_1(\tau) \end{cases} \tag{2.8}$$

and by solving the ODE, we obtain:

$$L_2(t) = \gamma(l - L_0)(t - \frac{\gamma l t^2}{2} + \gamma l \tau t + \frac{L_0 \tau^2 \gamma}{2} - L_0 \tau \gamma t) + c_2$$

and applying boundary conditions $L_2(\tau) = L_1(\tau)$, we obtain $c_2$:

$$c_2 = L_0 - \frac{\gamma^2\tau^2}{2}(l - L_0)^2$$

$$\boxed{L_2(t) = \gamma(l - L_0)t - \frac{\gamma^2 t^2}{2}(l - L_0)^2 + \gamma^2\tau t(l - L_0)^2 - \frac{\gamma^2\tau^2}{2}(l - L_0)^2 + L_0} \tag{2.9}$$

**Step 3.** On the time interval $[2\tau, 3\tau]$, $L(t-\tau) = L_(t-\tau)$, therefore:

$$\begin{cases} \dot{L_3}(t) = \gamma(l - L(t-\tau)) = \gamma(l - L_2(t-\tau)), & t \in [\tau.2\tau] \\ L_3(2\tau) = L_2(2\tau) \end{cases} \tag{2.10}$$

and by solving the ODE, we obtain:

$$L_3(t) = \gamma(l-L_0)t - \frac{\gamma t^2}{2}(l-L_0) + \gamma\tau t(l-L_0) + \frac{\gamma^2 t^3}{6}(l-L_0)^2 - \gamma^2\tau t^2(l-L_0)^2 + 2\gamma^2\tau^2 t(l-L_0)^2 + c_3$$

and applying boundary conditions, we compute $c_3$:

$$c_3 = L_0 - \frac{\gamma^2\tau^2}{2}(l - L_0)^2 - \frac{4\gamma^3\tau^3}{3}(l - L_0)^2$$

By using this method, it is possible to obtain an analytical solution to the DDE, but as it can be seen, it's a really long procedure if obtaining the solution over a long period of time is what is needed. Furthermore, studying the behaviour of this system using this functions is not the best option. Due to the limitations of this method,this solution was mainly used to check the accuracy of the numerical methods that were used after.

Plots showing examples of the results obtained with the step method are shown for different $\gamma$, $\tau$ values:

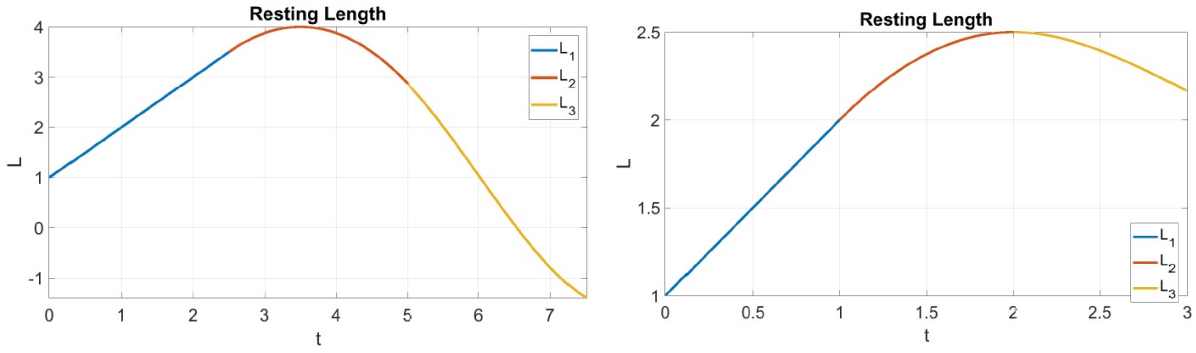


(a) Resting length $L(t)$ for $\gamma = 1$, $\tau = 2.5$.

(b) Resting length $L(t)$ for $\gamma = 1$, $\tau = 1$.

Figure 2.2: Resting length $L(t)$ obtained using Step Method.

### 2.2.2 Numerical approach

In this section, the numerical approach to the solution of this problem is explained. Methods that will be used are Forward Euler and Backward Euler. They might seem too simple al first glance, but they are both good enough for the accuracy needed, and they also have the advantage (in the case of the Backward Euler) that convergence is ensured if step size is sufficiently small.

#### Forward Euler Method

In order to solve problem (2.1) numerically, the Forward Euler method will be applied. The general procedure, for a given problem in the form $y'(t) = f(t, y(t)), \quad y(0) = y_0$, would be:

$$\begin{cases} Y_0 = \alpha \ \ (\textit{initial condition}) \\ Y_{i+1} = Y_i + h \ f(x_i, y_i) \end{cases}$$

where $\alpha$ is our initial condition, and $h$ the step size. In the case that this project tries to study, it should be taken into account that the equation (2.1) to be solved is a DDE, where the derivative depends on the function at previous times and therefore, delay needs to be taken into account.

To solve this issue regarding the delay, the proposed method is the following. Assuming that the delay $\tau$ is given, the step size will be $h = \dfrac{\tau}{n}$, $n \in \mathbb{N}$; resulting in the following Euler scheme;

$$\begin{cases} L_i = L_0, \quad i \in [0, n] \\ L_i = L_{i-1} + h(\gamma(l - L_{i-n})), \quad i > n \end{cases} \tag{2.11}$$

The algorithm, in pseudocode, is shown below:

(1) User input TN, the right-end-point of the interval where the equation will be solved $[0, TN]$.

(2) User input parameters TAU, GAMMA, l

(3) User input N

(4) User input history function L0

(5) Compute step size H=TAU/GAMMA

(6) Declare arrays T(N), L(N)

(7) Prefunction output

  (a) Loop 1

    (i) I = 1 to I = N+1

(ii) L(I) = L0

(b) End Loop 1

(8) Solution output

(a) Loop 2

(i) I = N+1 to I = N*TN/TAU

(ii) L(I) = L(I-1) + H*GAMMA*(l- L(I-N))

(b) End Loop 2

(9) END

which results, in Matlab code:

```
l = 2;
L0 = 1;     %history function
tn = 50; %observation time
gamma = 1;
tau = 1;

%% FORWARD EULER

n = 200;    %subdivisions
h = tau/n;
T = (-tau:h:tn)' ;
L = zeros(length(T),1);


for i = 1:(n+1)
    L(i) = L0;
end

for i = (n+1):length(L)
    L(i) = L(i-1) + h*(gamma*(l - L(i-n)));
end
```

Below, solutions for different $\gamma$ and $\tau$ values are shown:

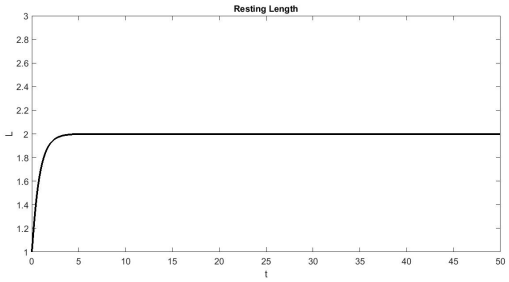


(a) Resting length for $\tau = 0.2$, $\gamma = 1$

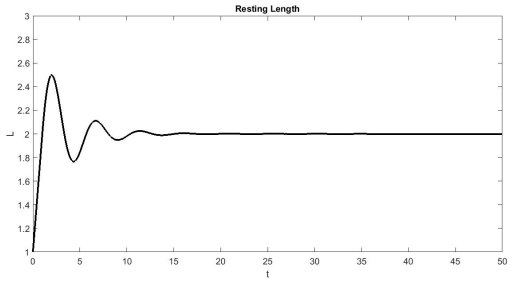


(b) Resting length for $\tau = 1$, $\gamma = 1$

Figure 2.3: Resting Length

In these figures, it can be observed that the behaviour of the oscillations is different for different $\gamma$ and $\tau$ values. In the following sections, this topic will be covered extensively.

Finally, the accuracy of this will be tested. Comparing to the solution obtained with the step method, which as stated before, is purely analytical and thus gives the exact solution. In the next figure, both solutions are plotted:

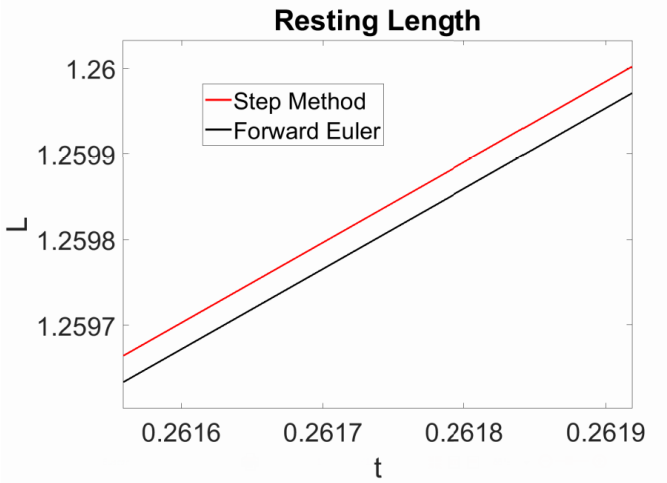


Figure 2.4: Difference between Step Method and Forward Euler for $\tau = 0.2$, $\gamma = 1$

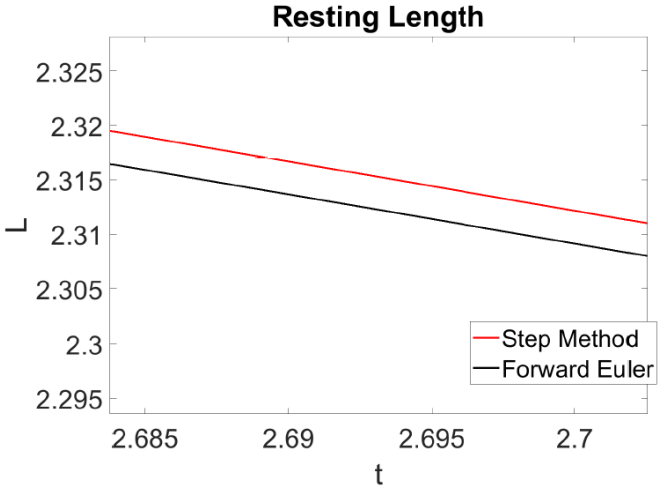


Figure 2.5: Difference between Step Method and Forward Euler for $\tau = 1$, $\gamma = 1$

From figures 2.4 and 2.5, it can be seen that the accuracy of the Forward Euler Method is enough. In this case, $n$ was set to 200 so precision was high enough for our calculations.

The relative error vs. step size plot is shown below, and as it can be seen, using a logarithmic scale, the resulting straight line has a 1/1 (approximately) slope, which is what could be expected from a first order method.

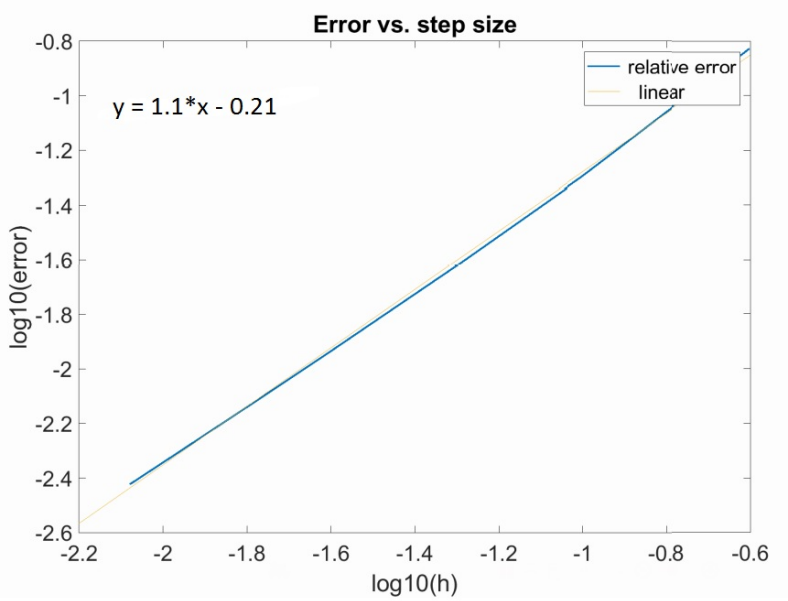


Figure 2.6: Relative error vs. step size. The resulting straight line has a 1/1 slope.

**Backward Euler**

The Backward Euler Method procedure reads:

$$\begin{cases} Y_0 = \alpha \ \ (initial\ condition) \\ Y_{i+1} = Y_i + h\ f(x_{i+1}, y_{i+1}) \end{cases}$$

which is an implicit method. But in our case, Backward Euler is not implicit because our derivative depends on the function which has a delay and therefore, being $h = \frac{\tau}{n}$ the step size, we have the following procedure:

$$\begin{cases} L_i = L_0, \quad i \in [0, n] \\ L_i i + 1 = L_i + h(\gamma(l - L_{i-n+1})), \quad i > n \end{cases} \tag{2.12}$$

As it can be observed, it is not an implicit method any more. Therefore, is almost the same as the Forward Euler Method with a slight difference, reason why the procedure was not used. Instead, the Forward Euler Method was the one chosen to simulate the system because of its simplicity and functionality.

## 2.3 Stability analysis for the 1-element model

In this section, the analysis of the behaviour of the system will be studied. As it can be deduced from figures 2.3a and 2.3b the behaviour of the oscillations changes when $\gamma$ and $\tau$ change, meaning that for low values no oscillations appear, and for high values, stability disappears. The objective of this part is to find critical values for $\gamma$ and $\tau$ for which oscillations appear, and critical values for which oscillations turn unstable.

This analysis will be conducted using the Method of Characteristics, which is briefly explained below and enables us to study the solution of the equation as a function of its parameters.

### 2.3.1 Method of Characteristics

It is a suitable method for studying simple cases like the one that is being treated. As an example, let the basic problem be:

$$y'(t) = a_1 y(t) + a_2(t - \delta) \tag{2.13}$$

and let us assume a solution that has the form $y(t) = Ce^{mt}$ with an arbitrary $C$ that can be computed afterwards using our initial conditions. Substituting $y(t)$ in 2.13, we get the characteristic equation:

$$mCe^{mt} = a_1 Ce^{mt} + a_2 Ce^{m(t-\delta)} \tag{2.14}$$

Finally, by finding the roots of equation 2.14 the solution of problem 2.13 can be found. Now, let the root $m$ be a complex number:

$$m = \alpha + i\beta$$

and therefore, the solution of equation 2.13 would be:

$$y(t) = Ce^{(\alpha+i\beta)t}$$

which, depending on the values of $\alpha$ and $\beta$, could be an oscillatory solution. The following cases could be distinguished:

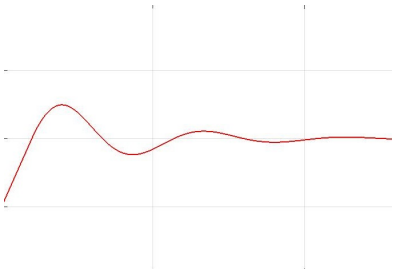

Figure 2.7: Stable oscillations.

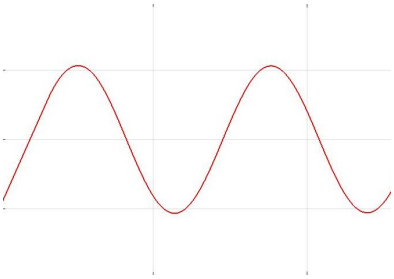

Figure 2.8: Sustained oscillations.

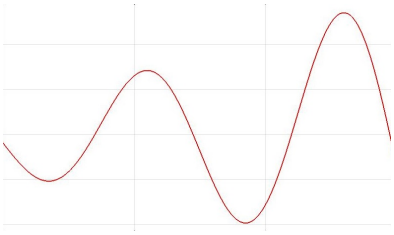

Figure 2.9: Unstable oscillations.

It is important to notice that problem (2.16) is a first order linear DDE, for which an exponential growth or decay solution could be expected. What is unexpected is that this first order equation has *oscillatory* solutions that depend on two parameters $\gamma, \tau$. This behaviour will be extensively analysed in the next sections by studying the values of $\alpha$ and $\beta$ as a function of $\tau$ and $\gamma$ and establishing for which values of them these different types of oscillations appear.

### 2.3.2 Characteristic equation

Now that the Characteristics Method has been introduced, the characteristic equation for the problem this project is about will be written. Let the BVP to be solved be:

$$\dot{L}(t) = \gamma(l - L(t-\tau)) \tag{2.15}$$
$$L(0) = L_0 \tag{2.16}$$

where $\gamma, \tau > 0$ and $l = L_0 + u = ct$. Then, let the solution be in the form:

$$L(t) = Ce^{mt} + l \tag{2.17}$$

where $C$ is an arbitrary constant. Substituting $L(t)$ in 2.16, we get:

$$mCe^{mt} = \gamma(l - (Ce^{m(t-\tau)} + l)) \tag{2.18}$$

Rearranging the terms, and dividing by $Ce^{mt}$, we get the following function of $m$, which needs to be equal to zero in order for 2.17 to be the exact solution:

$$\boxed{f(m) = me^{m\tau} + \gamma = 0} \tag{2.19}$$

Therefore, the characteristic equation of 2.16 reads:

$$\boxed{me^{m\tau} + \gamma = 0} \tag{2.20}$$

which is a function of $\tau$ and $\gamma$ parameters as well. Thus, we can study the values of $m$ as a function of them.

### 2.3.3 Roots of the Characteristic equation and general solution

In order to find the solution for (2.16), let $m$ be in the form:

$$m = \alpha + i\beta, \quad \alpha, \beta \in \mathbb{R}$$

Then, substituting $m$ in (2.20), we get:

$$(\alpha + i\beta)e^{(\alpha+i\beta)\tau} + \gamma = 0$$

separating real and imaginary parts of the equation, and taking into account that $e^{ix} = cos(x) + isin(x)$, we get the following system of equations:

$$\alpha cos(\beta\tau) - \beta sin(\beta\tau) = -\gamma e^{-\alpha\tau} \tag{2.21}$$
$$\alpha sin(\beta\tau) + \beta cos(\beta\tau) = 0 \tag{2.22}$$

which can be solved for $(\alpha, \beta)$. Another way of expressing these equations could be:

$$\alpha = -\beta cotg(\beta\tau) \tag{2.23}$$
$$\beta = \gamma sin(\beta\tau)e^{-\beta\tau cotg(\beta\tau)} \tag{2.24}$$

From equations (2.23) and (2.24), it can be deduced that the roots of the characteristic equation won't be unique, because of the periodic functions that are present, meaning that we would have an infinite number of $(\alpha, \beta)$ values for each $(\gamma, \tau)$. Therefore, the formal characteristic solution $L(t)$ is an infinite sum, which has the following form [16].

**Theorem**. *Let $\tau$ be any positive number, $\gamma$ any real non-zero number and $\alpha_i + i\beta$ complex roots obtained from (2.23) and (2.24), then, for $C_{1k}$ and $C_{2k}$ the function $L(t)$ defined as follows*

$$L(t) = C_0 e^{-t/\tau} + \sum_{k=1}^{\infty} C_i e^{m_k t} + \sum_{k=1}^{\infty} e^{\alpha_k t}(C_{1k} cos(\beta_k t) + C_{2k} sin(\beta_k t)) \tag{2.25}$$

*satisfies equation (2.16).*

As it has been stated, this is the general solution to the BVP problem (2.16), and many of the constants are equal to zero depending on the values of $\gamma$ and $\tau$. Therefore, here is the proof that equation (2.16) could have an oscillatory solution although it is a first order DDE.

### 2.3.4 Critical values for the appearance of oscillations

In this section, the values for $\gamma$ and $\tau$ for which oscillations appear are deduced. By studying equations (2.23) and (2.24), these values can be obtained.

First, let the equations be:

$$\alpha = -\beta cotg(\beta\tau) \tag{2.26}$$
$$\beta = \gamma sin(\beta\tau) e^{-\beta\tau cotg(\beta\tau)} \tag{2.27}$$

or, alternatively;

$$\alpha cos(\beta\tau) - \beta sin(\beta\tau) = -\gamma e^{-\alpha\tau} \tag{2.28}$$
$$\alpha sin(\beta\tau) + \beta cos(\beta\tau) = 0 \tag{2.29}$$

Now, let's study the value of $\alpha$ when $\beta$ is zero, which would give us no oscillations. From equation (2.23), where $\beta \neq 0$:

$$\lim_{\beta\to 0} \alpha = \lim_{\beta\to 0} -\beta\ cotg(\beta\tau) = \lim_{\beta\to 0} \frac{-\beta\tau\ cos(\beta\tau)}{\tau sin(\beta\tau)} = -\frac{1}{\tau} \tag{2.30}$$

Therefore, when $\beta \to 0$, we have $\alpha = -\frac{1}{\tau}$. Substituting this results in equation (2.28) when $\beta = 0$:

$$\alpha cos(\beta\tau) - \beta sin(\beta\tau) = -\gamma e^{-\alpha\tau} \Rightarrow -\frac{1}{\tau} = -\gamma e \Rightarrow \gamma\tau = \frac{1}{e} \tag{2.31}$$

The conclusions that can be drawn from this is that, given $\gamma, \tau > 0$, **no oscillations occur if** $\gamma\tau \in [0, \frac{1}{e}]$. This value for the product of these two parameters will be the first limit that separates different behaviours in the oscillations.

$$\boxed{(\gamma\tau)_{crit} = \frac{1}{e}} \tag{2.32}$$

Stability for the case $\gamma\tau < \frac{1}{e}$ is ensured. Given the fact that $\alpha = -\frac{1}{\tau}$ and $\tau > 0$, we have that $\alpha < 0$ if the parameters' value is within the two specified before, and this last condition is an indicator that the system is stable. Another way of expressing this stability condition is to say that if $\beta = 0$, then the system is stable.

Below, an example showing that there are no oscillations below these values are presented. The product of $\gamma,\ \tau$ is below $\frac{1}{e}$, and $l = 2$, $L_0 = 1$.

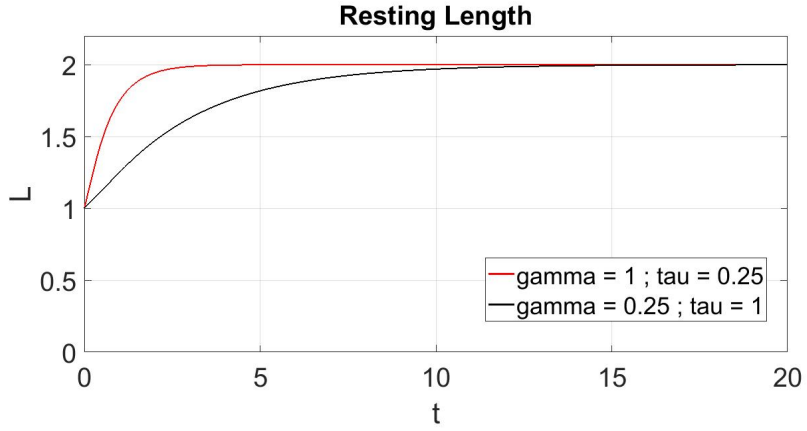


Figure 2.10: Solution with no oscillations for different $\gamma,\ \tau$ values, with $l = 2$ and $L_0 = 1$.

### 2.3.5 Critical values for instability

Now that the critical value for $\gamma$ and $\tau$ for which oscillations appear has been found, it's necessary to study the behaviour of the system. As it was stated before, we have two cases given $\beta \in \mathbb{R} - \{0\}$, plus the limit between them (sustained oscillations):

- Stable: $\alpha < 0$. Amplitude decreases.
- Sustained: $\alpha = 0$. Constant amplitude.
- Unstable: $\alpha > 0$. Increasing amplide.

Therefore, the objective of this section is to study the sign of $\alpha$ as a function of $\gamma,\ \tau$, analysis that can be carried by solving system (2.23)-(2.24) as a function of $\gamma,\ \tau$. Unfortunately, the analytical solution for this equations is not unique nor easy to find, so numerical methods will be needed if finding the roots is what we want.

Accordingly, the solutions $(\alpha, \beta)$ are the intersections between these two families of curves. In the next figures, plots of these two families of curves are shown, for $\gamma\tau > \frac{1}{e}$, along with the solution of the DDE.

$$\alpha = -\beta cotg(\beta\tau)$$
$$\beta = \gamma sin(\beta\tau)e^{-\beta\tau cotg(\beta\tau)}$$

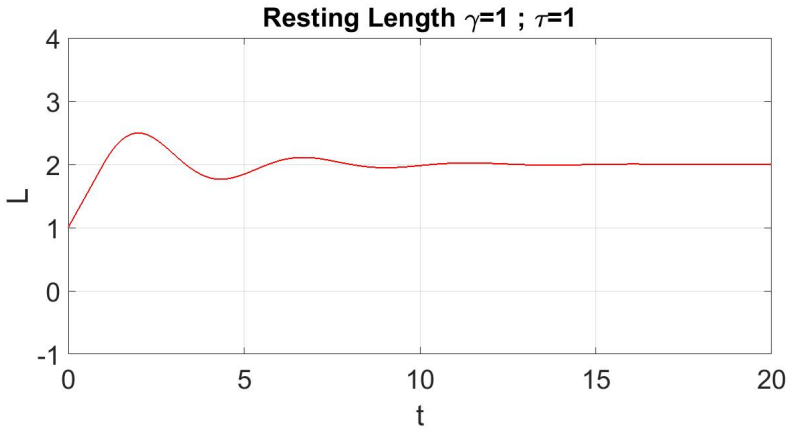


Figure 2.11: Resting length for $\tau = 1$ and $\gamma = 1$.

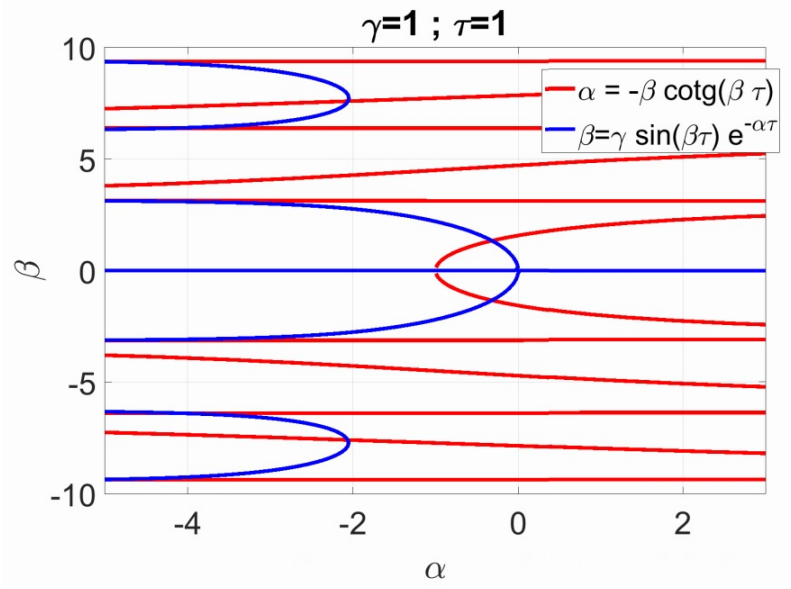


Figure 2.12: Intersections between the two curves for $\tau = 1$ and $\gamma = 1$.

As it can be observed in figure 2.12, for $\gamma = \tau = 1$, all intersections are negative, meaning that we have a negative value for $\alpha$ and therefore the system is stable. Now, if values for the product $\gamma\tau$ are higher, results change:

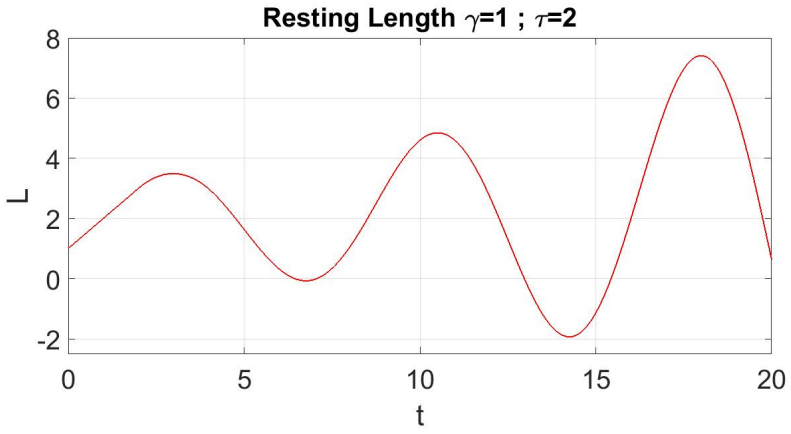


Figure 2.13: Resting length for $\tau = 2$ and $\gamma = 1$.

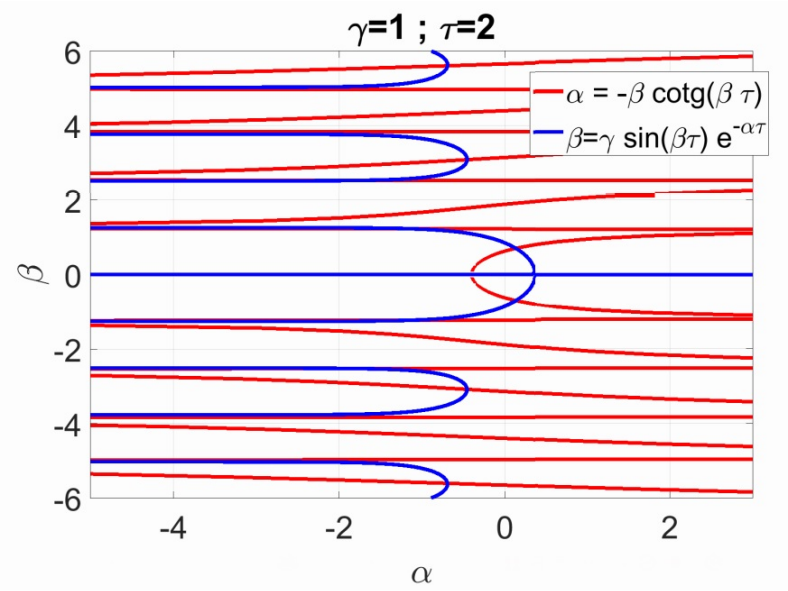


Figure 2.14: Intersections between the two curves for $\tau = 2$ and $\gamma = 1$.

In figure 2.14 we can see that roots have a positive $\alpha$ value, meaning that the system won't be stable, something that can be checked in figure 2.13. Therefore, from this results we can deduce that there is a limit for stability in the system, and it is a function of $\gamma$, $\tau$.

The limit between these two behaviours would be sustained oscillations, meaning that $\alpha \to 0$. From equation (2.23), we get;

$$0 = -\beta cotg(\beta\tau) \tag{2.33}$$

and since $\beta \neq 0$ because the case that is being studied is the one where oscillations are present and therefore our roots are complex, we get:

$$cotg(\beta\tau) = 0 \tag{2.34}$$

which is only satisfied if $\beta = \dfrac{\pi}{2\tau}$. Now, substituting in equation (2.24):

$$\beta = \gamma sin(\beta\tau)e^{-\alpha\tau} \Rightarrow \frac{\pi}{2\tau} = \gamma sin(\frac{\pi}{2}) \Rightarrow \frac{\pi}{2\tau} = \gamma \tag{2.35}$$

and the stability limit has been defined. Therefore, our second critical value for the product $\gamma\tau$ reads:

$$\boxed{(\gamma\tau)_{crit2} = \frac{\pi}{2}} \tag{2.36}$$

Graphical proof of this is shown below. In the following plots, different solutions for various ($\gamma$, $\tau$) values are presented. Each one illustrates a different oscillating behaviour (stable, sustained, unstable).

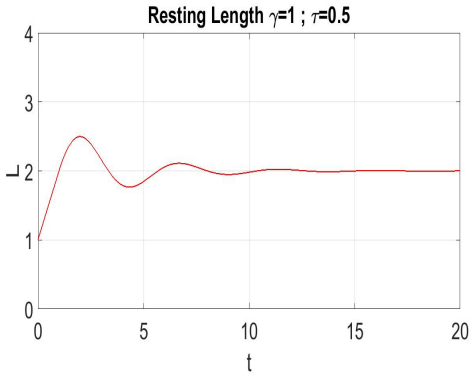


(a) Resting length $L(t)$ for $\gamma = 1$, $\tau = 0.5$.

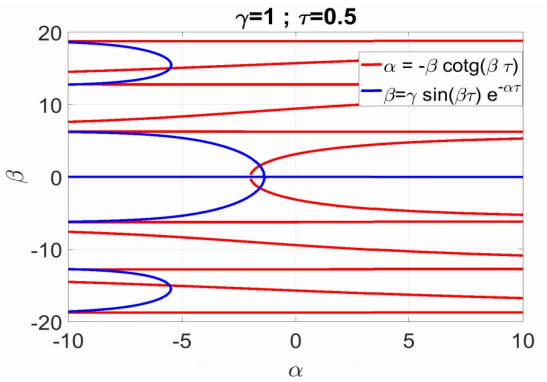


(b) Roots for $\gamma = 1$, $\tau = 0.5$. It can be seen that they are negative so the system is stable.

Figure 2.15: Resting Length and roots of characteristic equation for $(\gamma\tau) \in [\frac{1}{e}, \frac{\pi}{2}]$. Stable system.

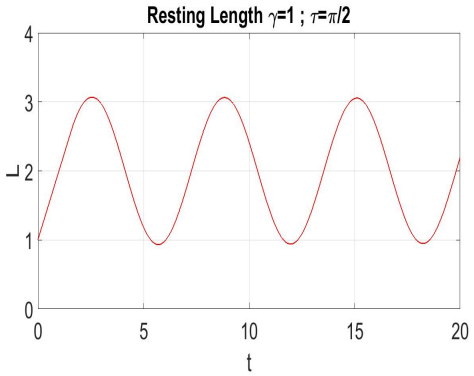


(a) Resting length $L(t)$ for $\gamma = 1$, $\tau = \frac{\pi}{2}$.

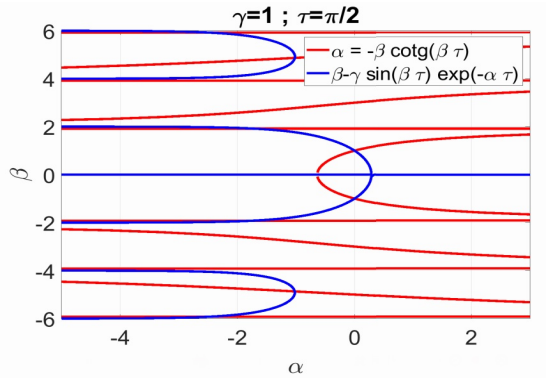


(b) Roots for $\gamma = 1$, $\tau = \frac{\pi}{2}$. It can be seen that $\alpha = 0$ so oscillations are sustained.

Figure 2.16: Resting Length and roots of characteristic equation for ($\gamma$, $\tau$) = $(1, \frac{\pi}{2})$. Sustained oscillations.

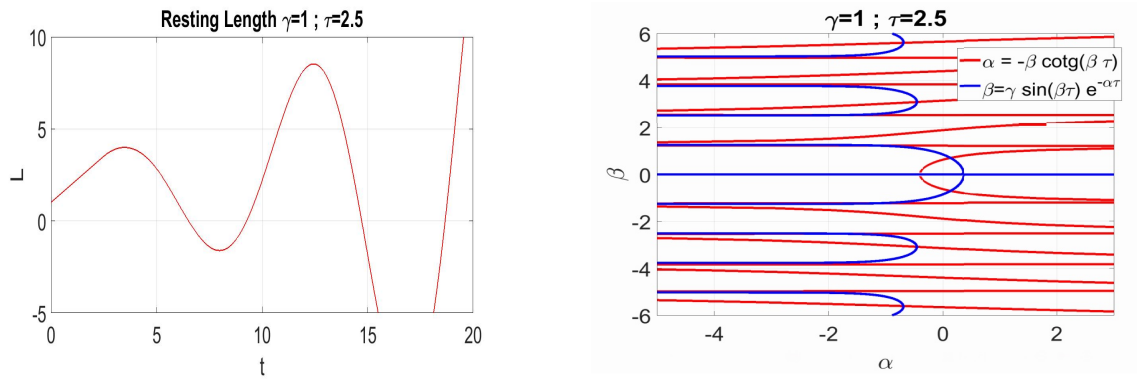


(a) Resting length $L(t)$ for $\gamma = 1$, $\tau = 2.5$. (b) Roots for $\gamma = 1$, $\tau = 2.5$. In this case, $\alpha > 0$.

Figure 2.17: Resting Length and roots of characteristic equation for $(\gamma,\ \tau) = (1, 2.5)$. Unstable oscillations.

Finally, the stability diagram for this 1-E system can be plotted in the $(\gamma, \tau)$ plane:

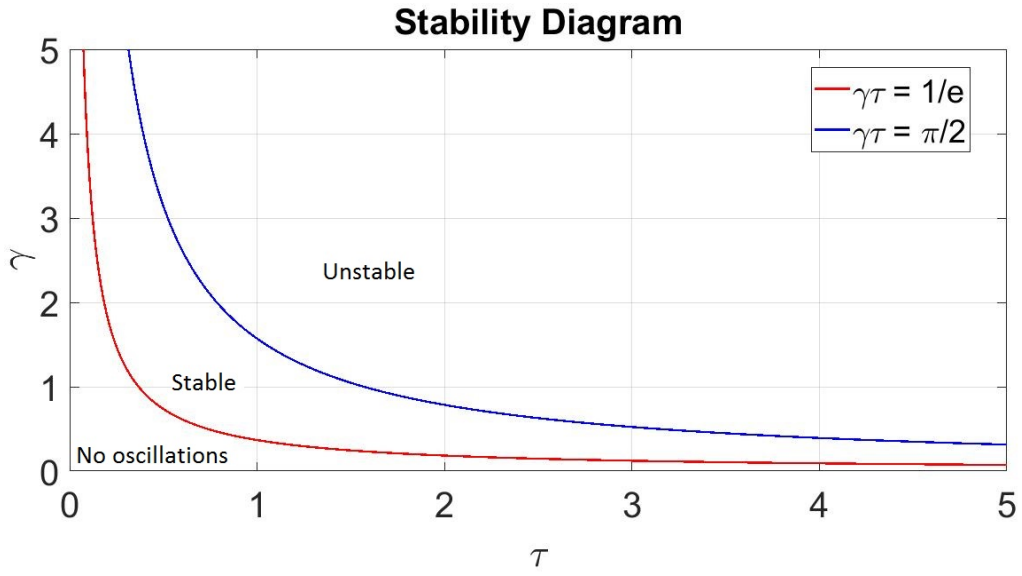


Figure 2.18: Stability diagram for the system.

## 2.4 Conclusion

Now that stability bound have been found and the fact that oscillations occur in this system, we can draw final conclusions to wrap everything up.

First conclusion to be drawn is that even though the equation that defines the BVP to be solved is a first order linear ODE, we have oscillations, probably due to the delay that the system presents. Not only numerical tests show that, but analytical tests too. By using the characteristics method, it has been proved that the solution can oscillate depending on the values of $(\gamma, \tau)$.

Secondly, it has been also shown that stability bounds exist for this system in particular ($(\gamma\tau)_{crit} = 1/e$ and $(\gamma\tau)_{crit2} = \pi/2$) , and it is also possible to have resonance

phenomenons in it. In addition, it is important to state that this resonance effects appear with no external forces being applied to the element, proof that the reason for the behaviour of the element might be coordinated by the mechanical equilibrium and the biological coupling that the system presents.

# Chapter 3

# 2-element model

In this chapter, the two element model is presented and analysed. First, numerical tests will be carried to check if behaviour is similar or equal to the one observed in chapter 2, and second, critical values for stability will be analytically deduced.

## 3.1 2-element problem statement

The model that is used in this case is also the Active Lengthening model [13]. Each element that composes the system follows the same equations as the element in chapter 2 (1-element model), but now, instead of applying a constant displacement $u$ at the end of the spring, a displacement $u(t)$ which is not necessarily constant will be applied at the contact point:

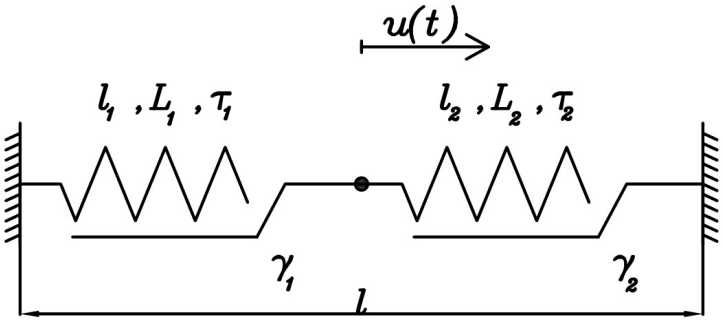


Figure 3.1: 2-element model.

*Notice that in this case, $L_{10} + L_{20} \neq l$, because $L_{i0}$, $i = 1, 2$ is their resting length (length when no stresses are applied on their ends) and in this case we have stresses at the contact point.*

In this problem, we have two equations, one for each spring, with their initial conditions, and two more equations which will be our kinematic conditions and equilibrium conditions. We will assume that each element has its $\gamma, \tau$ parameters, so equations are as follows:

$$\dot{L}_1(t) = \gamma_1(l_1(t - \tau_1) - L_1(t - \tau_1)) \tag{3.1}$$

$$\dot{L}_2(t) = \gamma_2(l_2(t - \tau_2) - L_2(t - \tau_2)) \tag{3.2}$$

where $L_1(t)$, $L_2(t)$ are each element's resting lengths and $l_1(t)$, $l_2(t)$ their current lengths. As for our conditions, we have kinematic conditions (3.5) (the sum of the current lengths must be equal to the total length $l$ of the system, as we are not allowing any movement on the ends), equilibrium conditions (3.4) ($\sigma$ must be the same at both springs at the point of contact between them), and initial conditions (3.3).

$$L_1(0) = L_{10}, \;\; L_2(0) = L_{20}, \;\; l_1(0) = l_{10}, \;\; l_2(0) = l_{20} \tag{3.3}$$
$$\sigma = k(l_1(t) - L_1(t)) = k(l_2(t) - L_2(t)) \tag{3.4}$$
$$l_1(t) + l_2(t) = l = ct \tag{3.5}$$

The main objective of this part will be to check if in this case each element behaves the same way as in the 1-element model, so results from chapter 2 can also be applied here.

## 3.2 System of equations

In this section, solutions for the 2-element problem will be presented. In this case, only numerical methods (Forward Euler) will be used due to the complexity that the system presents.

First of all, we will check if the two resting lengths of each elements have any relation between themselves. If we subtract equations (3.1) and (3.2), we get:

$$\dot{L}_1 - \dot{L}_2 = \gamma((l_1 - l_2) - (L_1 - L_2))$$

and using (3.4), we get:

$$\dot{L}_1(t) - \dot{L}_2(t) = 0 \Rightarrow \boxed{\dot{L}_1(t) = \dot{L}_2(t)} \tag{3.6}$$

Therefore, both elements change their resting length the same way, information that will help when checking if results make sense.

Secondly, we will write an expression for $l_1(t)$, $l_2(t)$ as a function of $L_1(t)$ and $L_2(t)$, so equations (3.1) and (3.2) will only have one unknown function and thus can be solved more easily using Forward Euler. To do so, $u(t)$ needs to be written as a function of the latter.

The relation between $l_i(t)$ and $u(t)$ is the following;

$$l_1(t) = l_{10} + u(t) \tag{3.7}$$
$$l_2(t) = l_{20} - u(t) \tag{3.8}$$

Therefore, if we combine equations (3.7) and (3.8), we get:

$$l_1(t) - l_2(t) = l_{10} - l_{20} + 2u(t)$$

and using equation (3.4):

$$L_1(t) - L_2(t) = l_{10} - l_{20} + 2u(t) \Rightarrow \boxed{u(t) = \frac{L_1(t) - L_2(t) - l_{10} - l_{20}}{2}} \tag{3.9}$$

Substituting $u(t)$ in equations (3.7) and (3.8), and taking into account that $l_{10} + l_{20} = l = ct$:

$$l_1(t) = \frac{l + L_1(t) - L_2(t)}{2} \tag{3.10}$$

$$l_2(t) = \frac{l - L_1(t) + L_2(t)}{2} \tag{3.11}$$

Finally, substituting (3.10) and (3.11) in (3.1) and (3.2):

$$\dot{L}_1(t) = \gamma_1 \frac{l - L_1(t - \tau_1) - L_2(t - \tau_1)}{2} \tag{3.12}$$

$$\dot{L}_1(t) = \gamma_2 \frac{l - L_1(t - \tau_2) - L_2(t - \tau_2)}{2} \tag{3.13}$$

Now, the system can be solved more easily using Forward Euler. Inputs for the problem are $L_1(t)$, $L_{10}$, $l_{i0}$, $\gamma_i$, $\tau_i$, $i = 1, 2$ and $L_{20}$ which is computed using the equilibrium condition $l_1 - L_1 = l_2 - L_2$. Outputs will then be $L_1(t)$, $L_2(t)$, $l_1(t)$, $l_2(t)$ and $u(t)$.

## 3.3 Numerical solutions

In this section, using the Forward Euler Method solutions to the system of equations (3.12)-(3.13) are found in order to check if behaviour varies from the one observed in the 1-element model. Numerical tests are carried on different cases where values for initial conditions vary from one to another. The Matlab code to obtain the latter was provided by Muñoz, J.

**Case 1.** $\tau_1 = \tau_2$**,** $\gamma_1 = \gamma_2$

In this case, both resting lengths oscillate the same way, and critical values are maintained (same $\tau_{crit1}$, $\tau_{crit2}$). This can also be deduced from equations (3.1) and (3.2), because if both expressions are combined:

$$\dot{L}_1(t) + \dot{L}_2(t) = \gamma(l - (L_1(t - \tau) + L_2(t - \tau))) \Rightarrow \dot{L} = \gamma(l - L(t - \tau))$$

which is the same equation treated in chapter 2. In the next figure, solutions for different $\gamma, \tau$ values are shown:

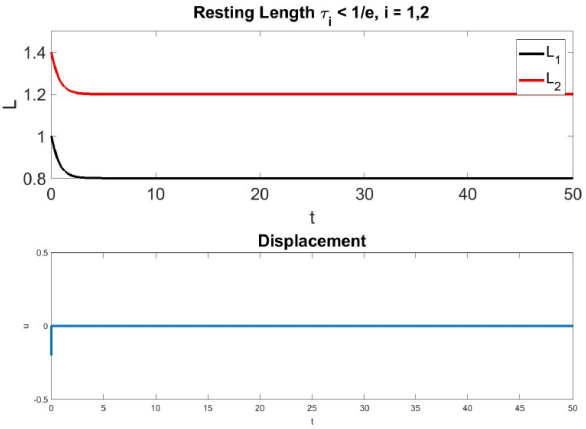


(a) Resting lengths for $\tau$ below $\tau_{crit1}$.

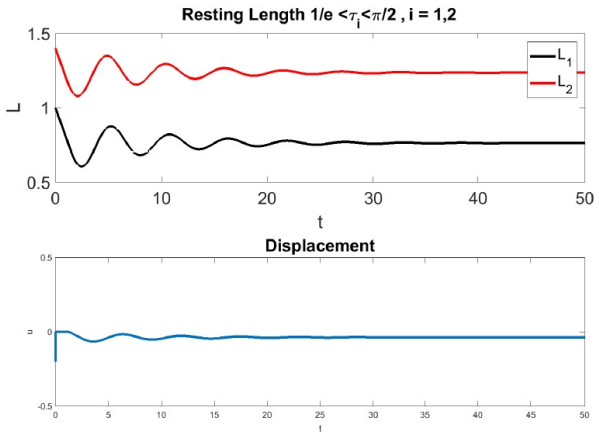


(b) Resting lengths for $\tau$ above $\tau_{crit1}$ and below $\tau_{crit2}$.

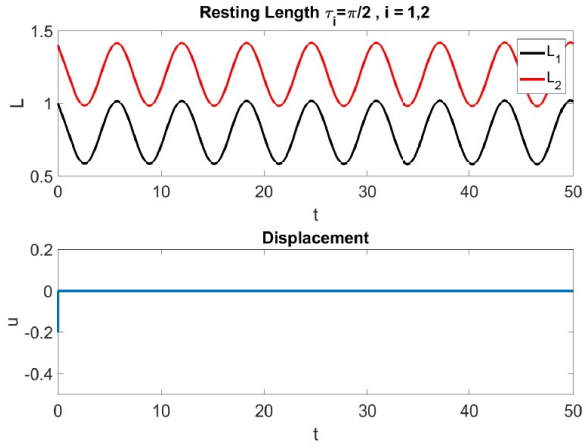


(c) Resting lengths for $\tau = \tau_{crit2}$

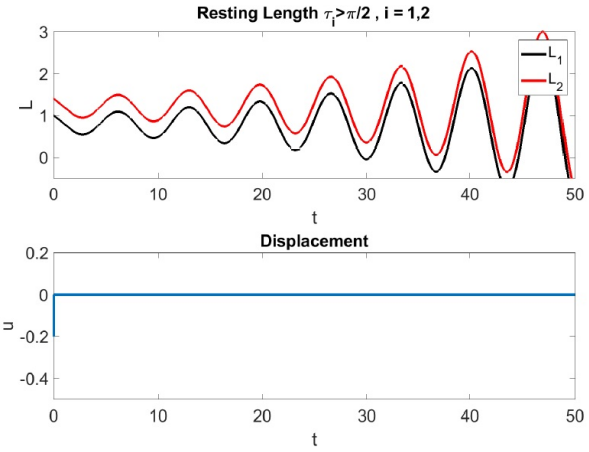


(d) Resting lengths for $\tau > \tau_{crit2}$

Figure 3.2: Resting lengths for case 1 (same $\tau$ and same $\gamma$.)

and as it can be observed, $u(t)$ does not oscillate because $L_1(t)$ and $L_2(t)$ are coupled, fact that was previously observed in equation (3.6) and implies that $L_1(t) = L_2(t) + ct$. Therefore, if resting lengths are equal but displaced with respect to the y axis, according to (3.9) $u(t)$ must be constant.

### Case 2. $\tau_1 \neq \tau_2$, $\gamma_1 = \gamma_2$

In this case, different combinations of values for $\tau_i$ have been tested. After these numerical tests were carried, some conclusions may be derived.

- If $\tau_1 > \tau_{crit_1}$ or $\tau_2 > \tau_{crit1}$, even if the other one is below the critical value, oscillations are observed in both elements, and in $u(t)$ as well (figure 3.3a).
- If $\tau_{crit1} < \tau_1,\ \tau_2 < \tau_{crit2}$, stable oscillations are observed in $L_1(t),\ L_2(t),\ u(t)$ (figure 3.3b).
- If $\tau_{crit1} > \tau_1,\ \tau_2$, no oscillations appear (figure 3.3c).
- If $\tau_1 > \tau_{crit_2}$ or $\tau_2 > \tau_{crit2}$, even if one of them is below the critical value for stable oscillations, unstable oscillations are observed in $L_1(t),\ L_2(t),\ u(t)$ (figure 3.3d).

- If $\tau_{crit2} < \tau_1,\ \tau_2$, unstable oscillations are observed in $L_1(t),\ L_2(t),\ u(t)$ (figure 3.3e).

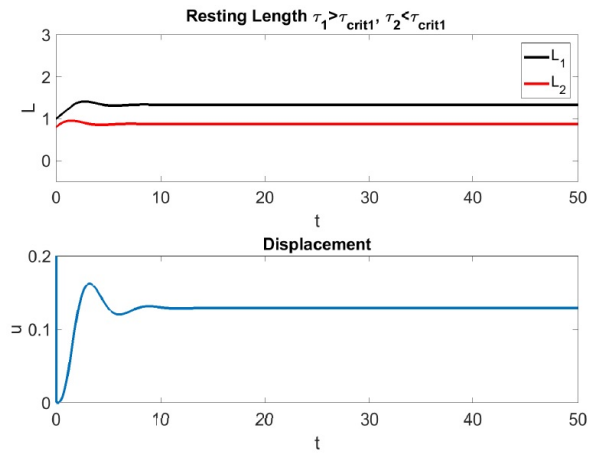


(a) $\tau_1 > \tau_{crit_1},\ \tau_2 < \tau_{crit1}$

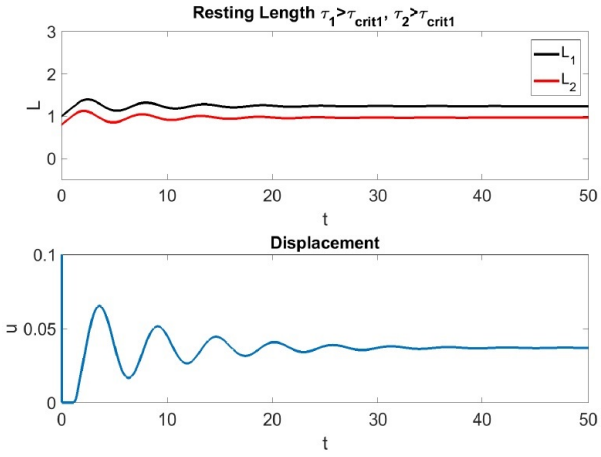


(b) $\tau_1 > \tau_{crit_1},\ \tau_2 > \tau_{crit1}$

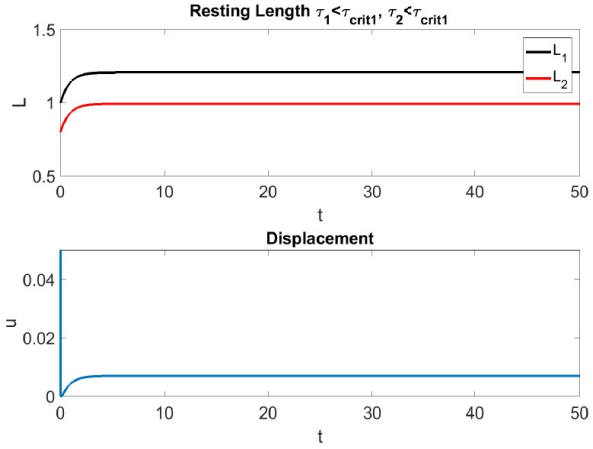


(c) $\tau_1 < \tau_{crit_1},\ \tau_2 < \tau_{crit1}$

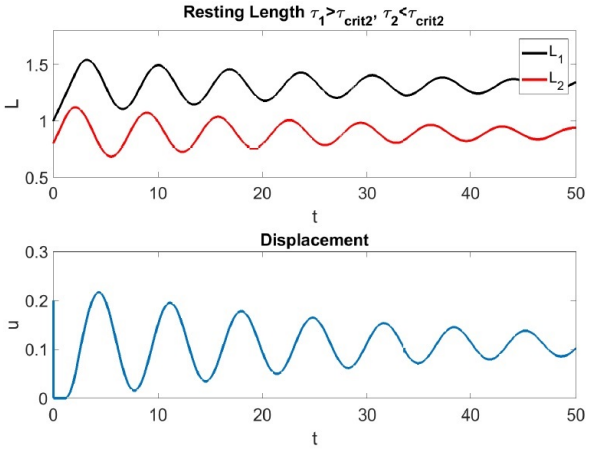


(d) $\tau_1 > \tau_{crit_2},\ \tau_2 < \tau_{crit2}$

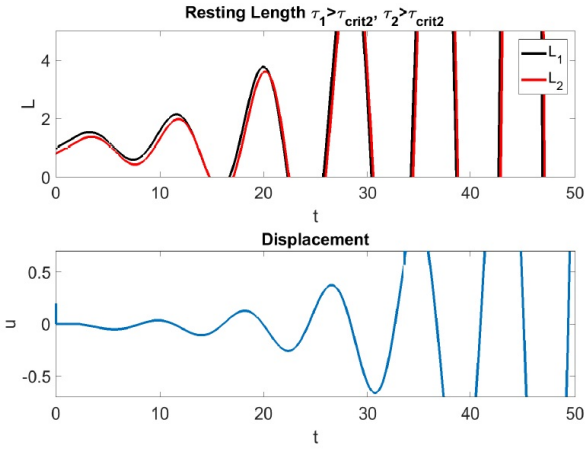


(e) $\tau_1 > \tau_{crit_2},\ \tau_2 > \tau_{crit2}$

Figure 3.3: Resting lengths for case 2 (different $\tau$ and same $\gamma$.)

Conclusions from this numerical tests are the following:

1. $u(t)$ only oscillates if $\tau_1 \neq \tau_2$. This is because oscillating phase depends on $\tau$, and from equation (3.9) it can be deduced that if delays are equal, $u(t)$ is constant.

2. Both resting lengths $L_i(t)$ behave equally (due to equilibrium equation (3.4)). Therefore, they probably have equal stability bounds.

3. Oscillations emerge even if one of the delays is below $\tau_{crit1}$, or they become unstable even if one of the values is below $\tau_{crit2}$, meaning that stability conditions may change slightly for the 2-element model. In the next section, this issue is addressed to check stability bounds for this model.

## 3.4 Stability analysis for the 2-element model

Stability analysis for this model will be done using Method of Characteristics, as it was done in chapter 2 for the 1-element model. In this case, the proposed solutions are the following;

$$L_1(t) = l_{10} + (L_{10} - l_{10})e^{m_1 t} \tag{3.14}$$
$$L_2(t) = l_{20} + (L_{20} - l_{20})e^{m_2 t} \tag{3.15}$$

and substituting in equations (3.12) and (3.13);

$$-m_1 l_{10} e^{m_1 t} = \frac{\gamma_1}{2}(l - (l_{10} + (L_{10} - l_{10})e^{m_1(t-\tau_1)}) - (l_{20} + (L_{20} - l_{20})e^{m_2(t-\tau_1)}))$$
$$-m_2 l_{20} e^{m_2 t} = \frac{\gamma_2}{2}(l - (l_{10} + (L_{10} - l_{10})e^{m_2(t-\tau_2)}) - (l_{20} + (L_{20} - l_{20})e^{m_2(t-\tau_2)}))$$

Taking into account that $l_1(t) - L_1(t) = l_2(t) - L_2(t)$, and dividing by $e^{m_1 t}$ and $e^{m_2 t}$ respectively each equation, we get;

$$m_1 = \frac{\gamma_1}{2}(e^{-m_1\tau_1} - e^{(m_2-m_1)t}e^{-m_2\tau_1})$$
$$m_2 = \frac{\gamma_1}{2}(e^{-m_2\tau_2} - e^{(m_1-m_2)t}e^{-m_2\tau_2})$$

Therefore, if (3.14) and (3.15) are exact solutions to the problem:

$$f_1(m_1, m_2) = m_1 + \frac{\gamma_1}{2}(e^{-m_1\tau_1} + e^{(m_2-m_1)t}e^{-m_2\tau_1}) = 0$$
$$f_2(m_1, m_2) = m_2 + \frac{\gamma_2}{2}(e^{-m_2\tau_2} + e^{(m_1-m_2)t}e^{-m_2\tau_2}) = 0$$

$f_1(m_1, m_2)$, $f_2(m_1, m_2)$ need to be equal to zero, and these equations are the ones that will provide stability conditions. Now, with with these equations, and taking into account that $m_1 = m_2 = m$ because these terms are time-independent [18], stability will now be given by expressions:

$$m + \gamma_1 e^{-m_1 \tau_1} = 0 \tag{3.16}$$
$$m + \gamma_2 e^{-m_2 \tau_2} = 0 \tag{3.17}$$

Numerically obtained stability diagrams are shown below;

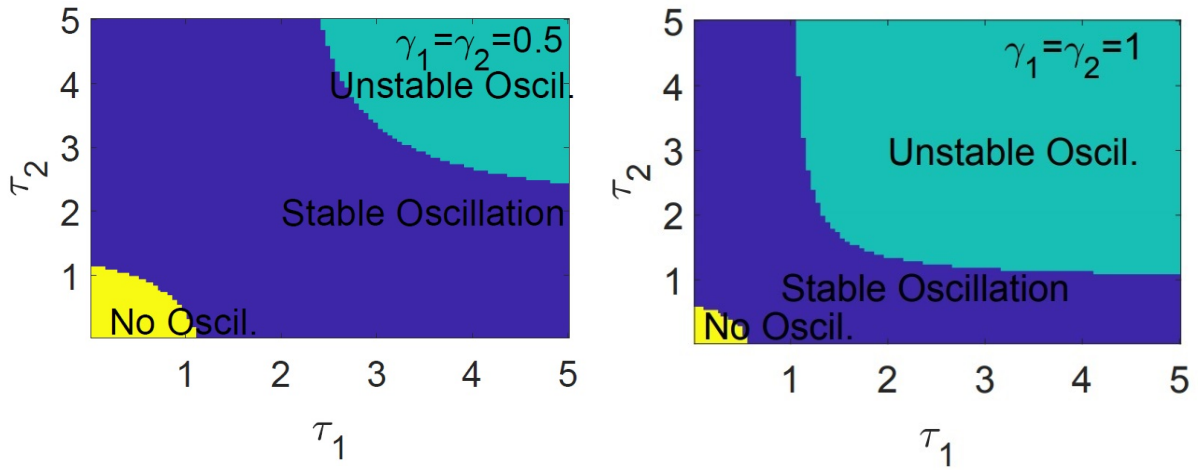


(a) Stability diagram for $\gamma_1 = \gamma_2 = 0.5$.

(b) Stability diagram for $\gamma_1 = \gamma_2 = 1$.

Figure 3.4: Stability diagrams for different $\gamma$ values. [18]

## 3.5 Conclusion

After analysing the 2-element model, it has been proved that it behaviour is really similar to the 1-element model and thus results obtained in the previous chapter were used. Even though, it is important to stress that in this case stability is given by the product between $\tau_1$ and $\tau_2$, which will give different stability diagrams for different pairs of $\gamma_1$, $\gamma_2$ values.

Another important conclusion that can be deduced from the previous analysis is that both elements behave the same way, meaning that equal stability conditions are present in the system. In other words, their behaviour is coupled, and same goes for displacement $u(t)$, which was expressed in terms of $L_1(t)$ and $L_2(t)$.

# Chapter 4

# Hybrid cell-centred/vertex model

In this chapter, the hybrid cell-centred/vertex model for multicellular systems developed by Muñoz, J., Rodríguez-Ferran, A. and Mosaffa, P. (2017) [17] is briefly explained. All ideas here presented can be found in [17].

As it has been mentioned in the introduction chapter, cell-based models can be described through cell-centred or vertex based models. In the first approach, the main scope is to establish forces between cell centres, and variations in the number of cells (cell proliferation or apoptosis) can easily be included. On the other hand, with the second approach cell-cell junction mechanics, which determine the emergent properties of tissues and monolayers, are described. The model that is now being described is a hybrid model that captures the advantages of both types, it defines cell-cell interactions between cell centres and but junction mechanics as well, but including the cell as an essential unit to ease transition in cell-cell contacts.

As this model is a hybrid one, two different networks which are coupled through a kinematic constraint that is allowed to relax progressively can be found:

- Triangular nodal network which represents cell centres (Delaunay triangulation of the cell-centres)
- Vertex network which represents cell boundaries (barycentric interpolation of vertices on cell boundaries.)

By using a variable resting length and applying Equilibrium Preserving Mapping on cell-cell connectivity which computes a new resting length that preserves nodal/vertex equilibrium, the change of this connectivity due to cell reorganisation or remodelling is adressed.

## 4.1 Tissue discretisation

Tissue kinematics are defined by the cell centers or nodes ($\boldsymbol{x}^i$) formed by a set of vertices ($\boldsymbol{y}^I$).Bar elements that define the networks are used to write the mechanical equilibrium equation.

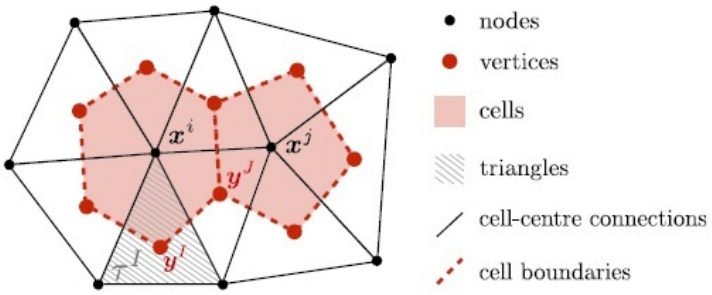


Figure 4.1: Discretisation of tissue into cell-centres (nodes, $\boldsymbol{x}^i$) and cell boundaries (vertices, $\boldsymbol{y}^I$). Nodal network and vertex network are outlined with continuous and dashed lines, respectively. [17]

To describe nodal geometry, it is assumed that a tissue forms a flat surface and has a constant number of nodes ($N_{nodes}$), which are kinematically described by their cell-centres positions $\boldsymbol{X} = \{\boldsymbol{x}^1, ...\boldsymbol{x}^{N_{nodes}}\}$ and connectivity $\boldsymbol{T}$ which define a triangulation of the domain. Position of the nodes will be found using mechanical equilibrium, and its connectivity using a Delaunay triangulation.

Vertex geometry description will start with the definition of the boundaries of the cells, which will be defined by a set of connected vertices $\{\boldsymbol{y}^1, ...\boldsymbol{y}^{N_{triangles}}\}$. A triangle will be associated to each vertice, and each interior node will be surrounded by a number of vertices which is not constant, nor in time, and nor from cell to cell.

Positions of vertices and nodes will be given by the interpolation:

$$\boldsymbol{y}^I = \sum_{i \in \tau} p^i(\boldsymbol{\xi}^I)\boldsymbol{x}^i \tag{4.1}$$

where $\boldsymbol{\xi}^I$ is a given parametric coordinate in a given triangle. Then, each two vertices $\boldsymbol{y}^I$ and $\boldsymbol{y}^J$ will be connected with a bar element if their corresponding triangle have a common edge. Positions and connectivity of the nodes and vertices is uniquely defined by $\boldsymbol{X}, \boldsymbol{T}$ and the local coordinates $\boldsymbol{\xi}^I$.

## 4.2 Mechanical equilibrium

Mechanical equilibrium of the bar elements that form nodal and vertex networks is computed by minimising the total elastic energy of the two networks. This minimisation problem leads to the equation:

$$\frac{\partial W_D(\boldsymbol{x})}{\partial \boldsymbol{x}^i} + \frac{\partial W_V(\boldsymbol{y}(\boldsymbol{x}))}{\partial \boldsymbol{x}^i} = \boldsymbol{0} \quad i = 1, ..., N_{nodes} \tag{4.2}$$

where $W_D(\boldsymbol{x})$ is the nodal network contribution to this energy, and $W_V(\boldsymbol{y}(\boldsymbol{x}))$ the vertex network contribution. Therefore, new nodal positions are found by minimising the total mechanical strain energy of the system, defined as $W_D(\boldsymbol{x}) + W_V(\boldsymbol{y}(\boldsymbol{x}))$.

$$\boldsymbol{x}^* = arg\, min_{\boldsymbol{x}}(W_D(\boldsymbol{x}) + W_V(\boldsymbol{y}(\boldsymbol{x}))) \tag{4.3}$$

which yields to the following equation:

$$\sum_{j\in S^i} \boldsymbol{t}_D^{ij} + \sum_{i\in B^i} p^i(\boldsymbol{\xi}^I)\boldsymbol{x}^i \sum_{J\in S^I} \boldsymbol{t}_V^{IJ} = \boldsymbol{0} \quad i = 1, ..., N_{nodes} \tag{4.4}$$

where $\boldsymbol{t}_D^{ij} = \dfrac{\partial W_D^{ij}}{\partial \boldsymbol{x}^i}$ represents the nodal traction at node $i$ due to bar $ij$, and $\boldsymbol{t}_V^{IJ} = \dfrac{\partial W_D^{IJ}}{\partial \boldsymbol{y}^I}$ are vertex tractions. Also, $B^i$ denotes the set of vertices that form the boundary of cell $i$ centred in $\boldsymbol{x}^i$, and $S^I$ is the set of vertices connected to vertex $I$.

Now, some constraints are added to the model. Cell volume invariance under tissue tension is relevant when size and number of cells is considered constant. Therefore, area constraint is imposed by adding the energy term $W_A(\boldsymbol{y}(\boldsymbol{x}))$, so now total energy of the system will be $W = W_D(\boldsymbol{x}) + W_V(\boldsymbol{y}(\boldsymbol{x})) + W_A(\boldsymbol{y}(\boldsymbol{x}))$, and the following term is added to equation 4.4:

$$\frac{\partial W_A}{\partial \boldsymbol{x}^i} = \frac{\lambda_A}{2}\boldsymbol{J} \sum_{m\in \bar{S}^i} (A^m - A^{m_0}) \sum_{IJ\in P^m} (p^i(\boldsymbol{\xi}^I)\boldsymbol{y}^J - p^i(\boldsymbol{\xi}^J)\boldsymbol{y}^I) \tag{4.5}$$

where $\lambda_A$ is a penalisation coefficient and $A_0^m$ and $A^m$ are initial and current areas of the cell respectively. $\bar{S}^i$ includes the nodes that surround node $i$ plus node $i$ itself, and $P^m$ denotes the segments of the polygon that surrounds node $\boldsymbol{x}^m$.

Finally, the last term that will be added is the $\xi$-relaxation. Initially, values of $\boldsymbol{\xi}^I$ are kept constant, meaning that vertices are not allowed to move from the barycentre, but if this constraint is disregarded, coordinates of those vertices will be treated as unknowns and therefore energy terms regarding the vertices are now dependant on those extra parameters. To address the problem, increments of $\boldsymbol{\xi}^I$ are limited between time steps, and a new term will be added to the total energy of the system:

$$W(\boldsymbol{x}, \boldsymbol{\xi}) = W_D(\boldsymbol{x}) + W_V(\boldsymbol{y}(\boldsymbol{x}, \boldsymbol{\xi})) + W_A(\boldsymbol{y}(\boldsymbol{x}, \boldsymbol{\xi})) + W_\xi(\boldsymbol{\xi}) \tag{4.6}$$

where

$$W_\xi(\boldsymbol{\xi}) = \frac{\lambda_\xi}{2} \sum_{I relaxed} ||\xi_{n+1}^I - \xi_n^I||^2 \tag{4.7}$$

and therefore, the final minimisation problem is:

$$\{\boldsymbol{x}^*, \boldsymbol{\xi}^*\} = argmin_{\boldsymbol{x},\boldsymbol{\xi}} W(\boldsymbol{x}, \boldsymbol{\xi}) \tag{4.8}$$

## 4.3 Equilibrium-Preserving Mapping

In order to include the ability to remodel that soft biological tissues present (to be able to change their neighbouring cells during growth, mobility, morphogenesis...) a new connectivity $\boldsymbol{T}_{n+1}$ needs to be computed after each time step $t_n$. But the redefinition of the network topology from $\boldsymbol{T_n}$ to $\boldsymbol{T_{n+1}}$ may involve drastic changes in the nodal and vertex equilibrium, and the new resting length $L^{ij}$ and $L^{IJ}$ are unknown for each new bar element. Therefore, the authors present an *Equilibrium-Preserving Mapping* that computes resting lengths by minimising the error of the mechanical equilibrium for the new connectivity. Two different approaches are considered: a map that preserves nodal and vertex

equilibrium in a coupled manner (*full network mapping*) and a map that preserves nodal and vertex equilibrium independently (*split-network mapping*). The latter is used when stresses in the nodal and vertex network follow different patterns.

The following images show the vertex distribution computed using this model for different $\gamma$ and $\tau$ values:

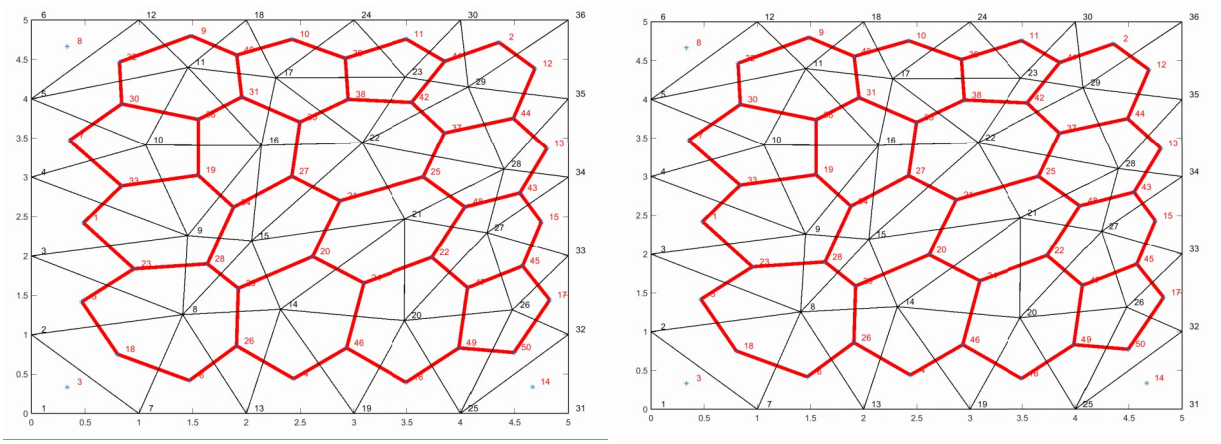

(a) Vertex distribution for $\gamma = 1$, $\tau = 0.2$

(b) Vertex distribution for $\gamma = 1$, $\tau = 0.2$

Figure 4.2: Vertex distribution computed using the hybrid model.[17]

## 4.4 Conclusion

What results from the combination of these equations and methods is the hybrid cell-centred/vertex discretisation for biological tissues, which allows to control both mechanical properties of cell boundaries and interior (cytoplasm) and therefore gives a complete description of cell movements. Such model can be applied to model tissue fluidisation or wound healing processes.

# Chapter 5

# Discussion

Up to here, one of the most important and surprising results that can be extracted from this analysis is that oscillations can emerge even if the equation that describes the system that is being studied is a first order linear ODE. Apparently, this type of equations do not generally provide an oscillating solution, but it has been proved that adding a time delay to the system results in an oscillating behaviour. Moreover, it has also been observed that even though no external forces were applied on the elements resonance effects appear and thus instability phenomenons emerge.

After these oscillating behaviour was observed the stability analysis was carried out, and results from this tests have shown that behaviour is characterized by the properties that each element presents. In the case of a single element, it has been proved that stability bounds exist and an analytical expression for them has been deduced, showing that they are a function of the delay that the system presents.

The analysis for the 2-element system provides additional conclusions as well. It has been proved that if both delays are equal, each element behaves exactly as the one studied in the previous case, with the same exact stability bounds. From this observations, it can be deduced that in this particular case, they are not affected by neighbouring elements and their length is constant (it was also proved that in this case displacement was constant). Different conclusions may be drawn from the case where delays were different for each element. Here it was observed that stability bounds depend on both element's parameters, meaning that each one is affected by their neighbours and therefore slightly changing stability conditions with respect to the single element model. But one thing is common in both cases. Resting lengths always have the same behaviour, meaning that they both oscillate in the same manner (same stability conditions). This is due to the equilibrium condition (3.4) that was imposed to write the equations for this case, which forces both to change their resting lengths to reach mechanical equilibrium.

Hence, with this Active Lengthening Model [13] which includes the chemical signalling delay that cells present, it is possible to properly simulate changes in the cytoskeleton and movements that were observed in the dorsal closure process of the *Drosophila melanogaster* embryo. Furthermore, it has also been proved that including this delay that represents the coupling between mechanical equilibrium and biological/chemical coupling, different types of oscillations emerge.

# Bibliography


[1] Farhadifar, R., Roper, J.C., Aigouy, B., Eaton, S., and Julicher, F. (2007) *The influence of cell mechanics, cell-cell interactions, and proliferation on epithelial packing.* Curr. Biol. 17, 2095-2104

[2] Harden, N. (2002) *Signaling pathways directing the movement and fusion of epithelial sheets: Lessons from dorsal closure in Drosophila.* Differentiation 70, 181-203

[3] Franke, J.D., Montague, R.A., and Kiehart, D.P. (2005) *Nonmuscle myosin II generates forces that transmit tension and drive contraction in multiple tissues during dorsal closure.* Curr. Biol. 15, 2208?2221

[4] Jankovics, F., and Brunner, D. (2006) *Transiently reorganized microtubules are essential for zippering during dorsal closure in Drosophila melanogaster.* Dev. Cell 11, 375-385

[5] Solon J., Kaya-Çopur A., Colombelli J., Brunner D. (2009) *Pulsed Forces Timed by a Ratchet-like Mechanism Drive Directed Tissue Movement during Dorsal Closure.* Cell 137, 1331-1342

[6] Bowden, L., Byrne, H., Maini, P., Moulton, D. (2016) *A morphoelastic model for dermal wound closure.* Biomech. Model. Mechanobiol., 15(3) , pp. 663-681

[7] Conte, V., Muñoz, J., Miodowink, M. (2008) *3D finite element model of ventral furrow invagination in the drosophila melanogaster embryo.* J. Mech. Behav. Biomed. Mater., 2 ,pp. 188-198

[8] Menzel, A., Kuhl, E. (2012) *Frontiers in growth and remodeling.* Mech. Res. Comm., 42 , pp. 1-14

[9] Davidson, L., Joshi, S., Kim, H., von Dassow, M., Zhang, J., Zhou, L. (2010) *Emergent morphogenesis: elastic mechanics of a self-deforming tissue.* J. Biomechanics, 43 , pp. 63-70

[10] Perrone, M., Veldhuis, J., Brodland, G. (2016) *Dynamic analysis of spatial flexible multibody systems using joint co-ordinates.* Biomech. Model. Mechanobiol., 15(2) , pp. 405-418

[11] Hardin, J., Walston, T. (2004) *Models of morphogenesis: the mechanisms and mechanics of cell rearrangement.* Curr. Opin. Genet. & Dev., 14(4) , pp. 399-406

[12] Bittig, T., Wartlick, O., Kicheva, A., Gonzalez-Gaitan, M., and Julicher, F. (2008) *Dynamics of anisotropic tissue growth.* New J. Phys. 10, 63001-63011

[13] Muñoz, J., Albo, S. (2013) *Physiology-based model of cell viscoelasticity.* PHYSICAL REVIEW E 88, 012708

[14] Salbreux, G., Charras, G., Paluch, E. (2012) *Actin cortex mechanics and cellular morphogenesis.* Trends in Cell Biol., 22(10) , pp. 536-545.

[15] Falbo, C.E. *Some Elementary Methods for Solving Functional Differential Equations.* Sonoma State University

[16] Falbo, C.E. (1995) *Analytic and numerical solutions to the Delay Differential Equation* $y'(t) = \alpha y(t-\tau)$. Joint Northern and Southern California Sections of the Mathematics Association of America

[17] Mosaffa, P., Rodríguez-Ferran A., Muñoz JJ. *Hybrid cell-centered/vertex model for multicellular systems with equilibrium-preserving remodelling.* Int J Numer Meth Biomed Engng. 2018;34:e2928. https://doi.org/10.1002/cnm.2928

[18] Muñoz J.J., Dingle M., Wenzel M. *Mass-less mechanical oscillations in biological tissues as a result of delay rest-length changes.* In preparation.